Intramolecular Radiative and Radiationless Charge Recombination Processes in Donor−Acceptor Carbazole Derivatives

Andrzej Kapturkiewicz,* Jerzy Herbich,* and Jerzy Karpiuk

Institute of Physical Chemistry Polish Academy of Sciences, Kasprzaka 44/52, 01-224 Warsaw, Poland

Jacek Nowacki

Department of Chemistry, Warsaw University, Pasteura 1, 02-093 Warsaw, Poland

Received: November 5, 1996[⊗]

Photoinduced intramolecular charge transfer (ICT) in a series of N-bonded donor−acceptor derivatives of 3,6-di-*tert*-butylcarbazole containing benzonitrile, nicotinonitrile, or various dicyanobenzenes as an electron acceptor has been studied in solutions. The latter group of compounds, contrary to benzonitrile and nicotinonitrile derivatives, shows a well-separated low-energy CT absorption band which undergoes a distinct blue shift with increasing solvent polarity. Solvatochromic effects on the spectral position and profile of the stationary fluorescence spectra clearly indicate the CT character of the emitting singlet states of all of the compounds studied both in a polar and a nonpolar environment. An analysis of the CT fluorescence and absorption band shapes leads to the quantities relevant for the electron transfer in the Marcus inverted region. The values of the fluorescence rate constants (k_f) and corresponding transition dipole moments (M) and their solvent polarity dependence indicate that the electronic coupling between the emitting ^{1}CT state and the ground state is a governing factor of the radiative transitions. The relatively large values of M indicate a nonorthogonal geometry of the donor and acceptor subunits in the fluorescent states. It is shown that Marcus theory can be applied for the quantitative description of the radiationless charge recombination processes in the cases when an intersystem crossing to the excited triplet states can be neglected.

1. Introduction

Over the past 30 years[1−32] there has been considerable interest in the photophysical properties of the donor (D)−acceptor (A) compounds formally linked by a single bond. Dual fluorescence of (*N*,*N*-dimethylamino)benzonitrile in a sufficiently polar and mobile environment, discovered by Lippert et al.,[1] has been discussed in terms of several models.[1−8] Grabowski and co-workers proposed that the primary excited state of D−A molecules (for example, 4-dialkylamino derivatives of benzonitrile,[4,9] benzaldehyde,[9,10] pyrimidines and pyridine[9,11,12]) converts to a highly polar fluorescent state with a mutually perpendicular conformation of the D^+ and A^- moieties. This twisted intramolecular charge transfer (TICT) state hypothesis predicts that the π-electronic decoupling of the D^+ and A^- subunits leads to a full charge separation and, consequently, to a large dipole moment and a considerable solvent reorientational energy (for reviews see refs 13−15). Dual luminescence is due to emission from the substrate and product of the excited state intramolecular electron transfer. The TICT fluorescence is strongly forbidden. It should be pointed out, however, that the role of the solvent and the changes of solute geometry are still a subject of controversy.[8,12,15−17]

A similar model has been adopted for large conjugate π-systems like biaryls (e.g., bianthryl[4,18]). These compounds,[18,19] as well as aryl derivatives of aromatic amines,[4,20−29] various derivatives of biphenyl,[12,30,31] and *N*-arylcarbazoles,[32] show a single fluorescence band at room temperature. The CT character of their fluorescent state in polar solvents seems to be well proved by the huge Stokes shift, the large dipole moment change upon excitation, and by the time-resolved fluorescence[21,22,25,26] and transient absorption studies.[23,24] There is an important difference between luminescence properties of these molecules and those containing 4-dialkylamino group as an electron donor—the CT fluorescence of the large conjugate D−A systems is strongly allowed. It has been postulated that the donor−acceptor conformation in the lowest excited singlet states of aryl derivatives of aromatic amines[28] and various derivatives of biphenyl[12] is far from perpendicular. Moreover, the temperature and solvatochromic effects on the band shape of the CT fluorescence show that the excited state conformation of *p*-anthryl derivatives of *N*,*N*-dimethylanilines is flattened with respect to that in the ground state.[28] Similarly, the luminescence properties of 4-(*N*,*N*-dimethylanilino)pyrimidine suggest an enhanced planarity of the ICT fluorescent state in a nonpolar environment.[12]

One of the most challenging problems is a large probability of the ^{1}CT → S_o emission in the latter D−A systems. It has been shown previously[27,28] that due to strong donor−acceptor interactions the simple perturbational approach underlying the theory of intermolecular π-complexes[33,34] can hardly be applied for the description of the photophysics of aryl derivatives of aromatic amines if the conformational changes are not taken into account. As a part of a continuing study, in this work we address the problems of molecular and electronic structure in a series of N-bonded D−A derivatives of 3,6-di-*tert*-butylcarbazole containing benzonitrile, nicotinonitrile, or various dicyanobenzenes as an electron acceptor (Figure 1) in order to understand the mechanism of the radiative and nonradiative transitions. The electron affinity of the acceptor moiety (increasing in the following order: benzonitrile, nicotinonitrile, dicyanobenzenes) and the position of the cyano group(s) with respect to the D−A bond (what induces a variety of the shapes of molecular orbitals and, consequently, changes the interactions

[⊗] Abstract published in *Advance ACS Abstracts,* February 15, 1997.

S1089-5639(96)03456-1 CCC: $14.00

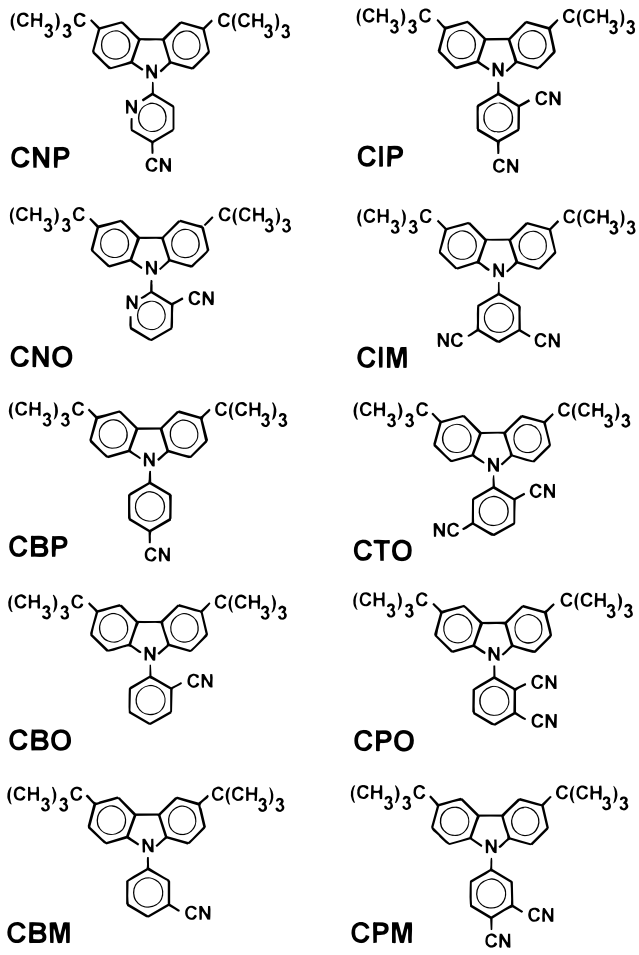

Figure 1. Formulas of electron donor−acceptor derivatives of 3,6-di-*tert*-butylcarbazole and their abbreviations used in the text.

between the donor and acceptor subunits) are the main variables in our comparative investigations.

The presented results are based on a study of the solvent and temperature effects on the spectral position and the band shape of the CT absorption and fluorescence spectra as well as on the CT emission quantum yields and excited state depopulation kinetics.

2. Experimental Section

2.1. Materials. The synthesis and purification of 3,6-di-*tert*-butylcarbazole (CAR) and its electron donor−acceptor derivatives: 4-(3,6-di-*tert*-butylcarbazol-9-yl)benzonitrile (CBP), 3-(3,6-di-*tert*-butylcarbazol-9-yl)benzonitrile (CBM), 2-(3,6-di-*tert*-butylcarbazol-9-yl)benzonitrile (CBO), 6-(3,6-di-*tert*-butylcarbazol-9-yl)nicotinonitrile (CNP), 2-(3,6-di-*tert*-butylcarbazol-9-yl)-nicotinonitrile (CNO), 3-(3,6-di-*tert*-butylcarbazol-9-yl)phthalonitrile (CPO), (3,6-di-*tert*-butylcarbazol-9-yl)terephthalonitrile (CTO), 4-(3,6-di-*tert*-butylcarbazol-9-yl)phthalonitrile (CPM), 4-(3,6-di-*tert*-butylcarbazol-9-yl)isophthalonitrile (CIP), and 5-(3,6-di-*tert*-butylcarbazol-9-yl)isophthalonitrile (CIM) will be described elsewhere.[35]

n-Hexane (HEX), methylcyclohexane (MCH), butyl ether (BE), isopropyl ether (IPE), ethyl ether (EE), butyl acetate (BA), ethyl acetate (EA), tetrahydrofuran (THF), 1,2-dichloroethane (DCE), *N*,*N*-dimethylformamide (DMF), acetonitrile (ACN), and dimethyl sulfoxide (DMSO) were of spectroscopic or fluorescence grade. Butyronitrile, BN, (Merck, for synthesis) was triply distilled over $KMnO_4$+K_2CO_3, P_2O_5, and CaH_2, respectively. All solvents did not show any traces of luminescence. The solutions were deaerated by the saturation with preliminary purified and dried argon for fluorescence quantum yield and lifetime measurements as well as for electrochemical investigations.

2.2. Instrumentation and Procedures. Absorption spectra were recorded with a Shimadzu UV 3100 spectrometer and corrected luminescence and excitation spectra by means of the Jasny spectrofluorimeter.[36] Quinine sulphate in 0.1 N H_2SO_4 served as a quantum yield standard ($\Phi_f = 0.51$).[37]

Fluorescence lifetimes were determined using the sampling technique with the excitation provided by a MSG 350S nitrogen laser (with pulse duration of 0.6 ns (fwhm)).[38] The experimental decay curves were analyzed by the single-curve method using the DECAN deconvolution program (kindly obtained from Prof. F. C. De Schryver, Catholic University of Leuven, Belgium) with the reference convolution based on the Marquardt algorithm;[39] the χ^2 test and the distribution of residuals served as the main criteria in the evaluation of fit quality. In all the cases studied the fluorescence decay was monoexponential on the nanosecond scale of observation.

The standard potentials of the one electron oxidation E_{ox}(D) and reduction E_{red}(A) of all the compounds studied were determined by a cyclic voltammetry technique. Measurements were performed in ACN containing 0.1 M tetra-*n*-butylammonium hexafluorophosphate ($TBAPF_6$) as the supporting electrolyte. Investigation of the stability of the electrogenerated radical ions have been made by varying the scan rate. The analysis of the voltammograms, recorded at scan rates fast enough to minimize the influence of the radical ions instabilities, allowed us to determine the standard redox potentials. The details of instrumentation used have been described previously.[40,41]

Semiempirical quantum chemical calculations have been performed using the AM1 method (from HYPERCHEM package developed by Hypercube Inc.). Ground state geometry optimizations were also done by molecular mechanics (MMX force field, PCMODEL from Serena Software). Other calculations (e.g., band shape analysis) were made by means of the least-squares method using a Sigma Plot package from Jandel Corp.

3. Results and Discussion

3.1. Absorption and Fluorescence. Room temperature absorption spectra of the studied compounds are presented in Figures 2 and 3. The spectra show a superposition of the bands corresponding to the donor and acceptor subunits which seem to be only slightly perturbed by their interactions. Similarly to carbazole,[42−44] the first five absorption bands of CAR, being centered in *n*-hexane at 29 700, 33 800, 38 800, 40 200, and 43 100 cm^{-1}, have been assigned to the final $^1(\pi,\pi^*)$ states of $^1A_1$, $^1B_2$, $^1B_2$, $^1A_1$, and $^1B_2$ symmetry, respectively. The two former bands correspond in Platt's notation to the ^1L_b and ^1L_a excited states, and the last one to the ^1B_a state. The transitions with a relatively high probability ($^1L_a \leftarrow S_o$ and $^1B_a \leftarrow S_o$) can be clearly observed in the absorption spectra of all the compounds studied.

The effect of the lowest transitions in the acceptor moieties,[45,46] $^1L_b \leftarrow S_o$ (centered at 35 000−38 000 cm^{-1} with the molar extinction coefficients ϵ_m in the range of 500−2500 M^{-1} cm^{-1}) and $^1L_a \leftarrow S_o$ (centered at 41 000−46 000 cm^{-1} with ϵ_m in the range of 7000−25 000 M^{-1} cm^{-1}), is manifested by an increase of the width and intensity of the second and third absorption bands of the D−A molecules with respect to those of CAR. In the case of dicyano derivatives (CIM, CIP, CPO, and CPM) an additional band (most probably corresponding to the batochromically shifted $^1B_a \leftarrow S_o$ transition in the acceptor

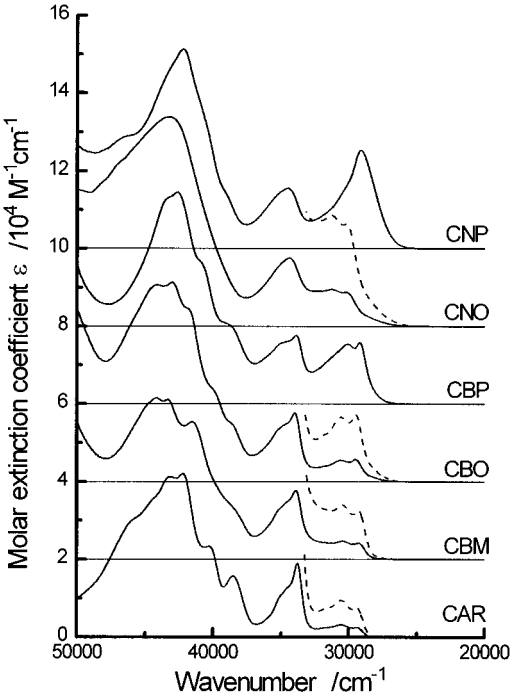

Figure 2. Room temperature absorption spectra recorded in acetonitrile for 3,6-di-*tert*-butylcarbazole (CAR) and its donor−acceptor derivatives containing benzonitrile (CBM, CBO, and CBP) and nicotinonitrile (CNO and CNP) as an electron acceptor. Spectra of CBM, CBO, CBP, CNO, and CNP are shifted along the *y*-axis by a factor of 2×10^4. Low-energy parts of the absorption spectra of CAR, CBM, CBO, and CNO are expanded by a factor of 3.

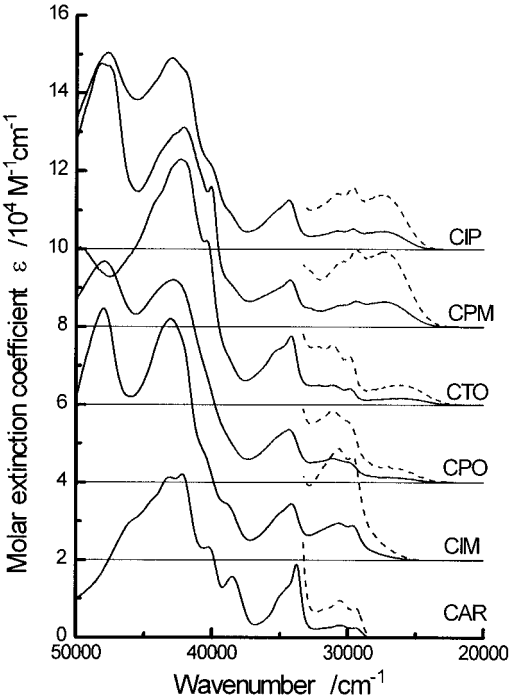

Figure 3. Room temperature absorption spectra recorded in acetonitrile for 3,6-di-*tert*-butylcarbazole (CAR) and its donor−acceptor derivatives containing phthalonitrile (CPO and CPM), isophthalonitrile (CIM and CIP) and terephthalonitrile (CTO) as an electron acceptor. Spectra of CIM, CPO, CTO, CPM, and CIP are shifted along the *y*-axis by a factor of 2×10^4. Low-energy parts of the absorption spectra are expanded by a factor of 3.

moiety) with the high intensity ($\epsilon_m \approx 60\,000$ M^{-1} cm^{-1}) is observed at about 48 000 cm^{-1}.

Detailed inspection of the low-energy absorption region of the D−A carbazole derivatives containing benzonitrile and nicotinonitrile as an electron acceptor clearly indicates the presence of additional charge transfer singlet states. A long wave shoulder attributed to the $^1CT \leftarrow S_o$ transition is observed in CBO and CNO (Figure 2). A dramatic increase of the intensity of the first absorption maximum of CBP[32] and CNP indicates that two transitions $^1CT \leftarrow S_o$ and $^1(\pi,\pi^*) \leftarrow S_o$ are superimposed in this band. The red shift of the CT absorption band in CBO and CNO (as compared with CBP and CNP) may be explained by an increase of the coulombic stabilization energy in a corresponding radical ion pair $A^- - D^+$ with respect to that in the latter ones (arising from the position of the negatively charged CN group versus the positively charged donor moiety). Due to the increasing electron affinity of the acceptor subunit and the corresponding lowering of the CT states energy, (3,6-di-*tert*-butylcarbazol-9-yl)dicyanobenzenes (except CIM) show a well-separated low-energy CT absorption band (Figure 3).

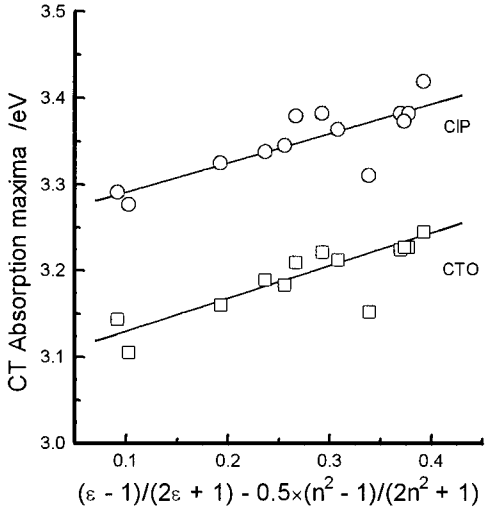

Figure 4. Plot of the solvatochromic shift of the energy related to the CT absorption maxima for CTO and CIP (see text). The solvent polarity function corresponds to eq 1.

An interesting result is provided by the blue shift of the CT absorption bands with increasing solvent polarity (Figure 4). Such an anomalous solvatochromic effect on the spectral position of the CT absorption spectra of the bichromophoric compounds connected by a single bond has been observed previously.[32,47]

According to the theory of dielectric polarization,[48] one can expect the opposite behavior of the absorption band corresponding to the transition from a state with a small dipole moment to a state with a large one (eq 1). Assuming a point dipole situated in the center of the spherical cavity and neglecting the mean solute polarizability α in the states involved in the transition ($\alpha \cong \alpha_e \cong \alpha_g \cong 0$), one obtains[49−51]

$$hc\tilde{\nu}_{abs} \cong hc\tilde{\nu}_{abs}^{vac} - \frac{2\vec{\mu}_g(\vec{\mu}_e - \vec{\mu}_g)}{a_o^3}\left[\frac{\epsilon - 1}{2\epsilon + 1} - \frac{1}{2}\frac{n^2 - 1}{2n^2 + 1}\right] \quad (1)$$

where $\vec{\mu}_g$ and $\vec{\mu}_e$ are the dipole moments of the solute in the ground and excited state, correspondingly, ν_{abs} and $\tilde{\nu}_{abs}^{vac}$ are the spectral positions of a solvent-equilibrated absorption maxima and the value extrapolated to the gas-phase, respectively, a_o is the effective radius of the Onsager cavity,[52] and ϵ and n are the static dielectric constant and the refractive index of the solvent, respectively. In the case of the well-separated CT absorption bands, eq 1 is used to determine the values of $\vec{\mu}_g(\vec{\mu}_e - \vec{\mu}_g)/a_o^3$ and $\tilde{\nu}_{abs}^{vac}$. The increase of the energy $hc\tilde{\nu}_{abs}$ in polar solvents, however, can be hardly explained within the Onsager−Lippert−Mataga model; eq 1 predicts either (i) the opposite orientation

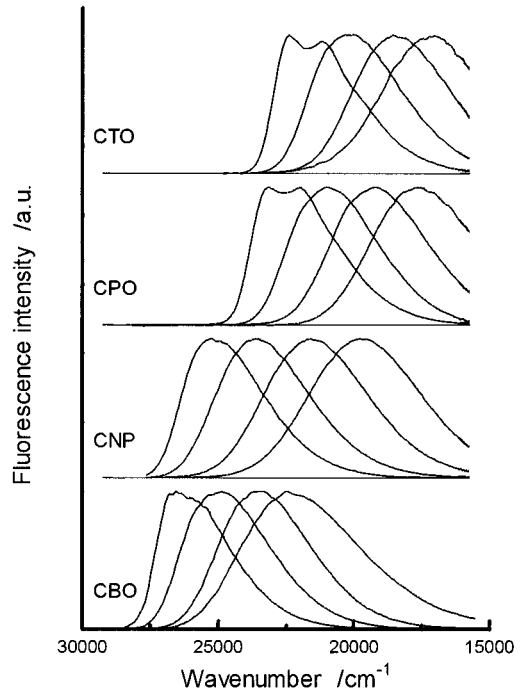

Figure 5. Corrected and normalized fluorescence spectra of CBO, CNP, CPO, and CTO in *n*-hexane, butyl ether, tetrahydrofuran, and acetonitrile (from left to right, respectively).

of the dipole moments $\vec{\mu}_g$ and $\vec{\mu}_e$ (it can explain the observed effects for CBO and CNO but surely not for the other compounds studied; e.g., this effect is also observed for CTO with $|\vec{\mu}_g|$ as small as about 1 D) or (ii) that the absolute values of $|\vec{\mu}_e|$ are much lower than those of $|\vec{\mu}_g|$ which would be in a striking contrast with the solvatochromic effects on the fluorescence spectra (Figure 5). The blue shift of the CT absorption bands of the large aromatic systems is probably due to the fact that the dipolar molecule cannot be approximated by the point dipole situated in the center of the cavity (see Appendix). In our case the ground state dipole moment is mostly determined by cyano groups lying far from the center of the molecule. It leads to an increase of the effective Onsager reaction field[48] and to a corresponding increase in the ground state solvation energies, and, consequently, to the observed blue shift in the absorption spectra. The approximation of the spherical cavity, however, with the dipole moment situated in its center seems to be more appropriate for the excited state, in which the negative and positive ends of the electric dipole are localised nearly in the centers of the A and D subunits, respectively.

Solvent effects on the room temperature fluorescence spectra of the donor−acceptor carbazole derivatives are presented in Figure 5. A considerable red shift of their spectral position, and the increase of the Stokes shift and of the emission bandwidth with increasing solvent polarity point to the CT character of the fluorescent states and clearly indicate that the absolute values of $|\vec{\mu}_e|$ are much higher than those of $|\vec{\mu}_g|$.

The excited state dipole moments $\vec{\mu}_e$ can be estimated by the fluorescence solvatochromic shift method[49−51] due to the fact that, in our case, the excited states live sufficiently long with respect to the orientational relaxation time of the solvent. Under the same assumptions as used for expression 1, it follows that

$$hc\tilde{\nu}_{flu} \cong hc\tilde{\nu}_{flu}^{vac} - \frac{2\vec{\mu}_e(\vec{\mu}_e - \vec{\mu}_g)}{a_o^3}\left[\frac{\epsilon - 1}{2\epsilon + 1} - \frac{1}{2}\frac{n^2 - 1}{2n^2 + 1}\right] \quad (2)$$

where $\tilde{\nu}_{flu}$ and $\tilde{\nu}_{flu}^{vac}$ are the spectral positions of the solvent-equilibrated fluorescence maxima and the value extrapolated

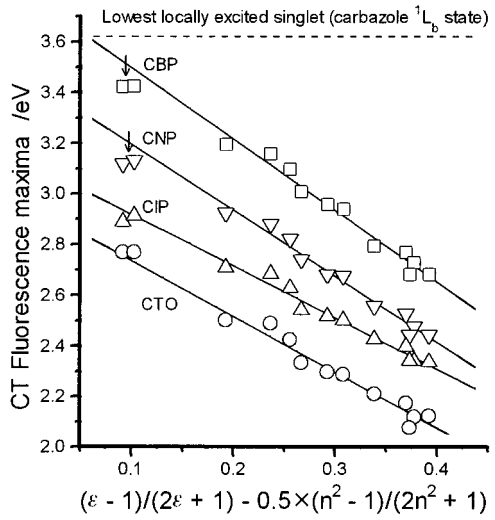

Figure 6. Solvatochromic shift of the energy related to the CT fluorescence maxima for CTO, CIP, CNP, and CBP as a function of the solvent polarity corresponding to eq 2. The arrow indicates the deviation in nonpolar solvents from the linear correlation observed in polar media.

TABLE 1: Slopes and Intercepts of the Solvatochromic Plots of the CT Fluorescence of the D−A Carbazole Derivatives

	nonpolar and polar solvents[a]		polar solvents only[b]	
compound	$hc\tilde{\nu}_{flu}^{vac}$, eV	$\vec{\mu}_e(\vec{\mu}_e - \vec{\mu}_g)/a_o^3$, eV	$hc\tilde{\nu}_{flu}^{vac}$, eV	$\vec{\mu}_e(\vec{\mu}_e - \vec{\mu}_g)/a_o^3$, eV
CNO	3.11	0.83	3.22	1.00
CBO	3.47	0.94	3.58	1.10
CPO	3.08	1.16	3.16	1.27
CTO	2.98	1.14	3.01	1.17
CIP	3.10	0.98	3.16	1.07
CBM	3.69	1.29	3.82	1.49
CBP	3.71	1.29	3.85	1.51
CNP	3.38	1.18	3.51	1.37
CIM	3.13	1.16	3.25	1.35
CPM	3.27	1.45	3.42	1.69

[a] Fit of the CT fluorescence maxima to eq 2 in the whole range of the solvents used (including methylcyclohexane and *n*-hexane). [b] Fit of the CT fluorescence maxima to eq 2 in polar solvents (from butyl ether to acetonitrile).

to the gas-phase, respectively. The compounds studied show a satisfying linear correlation between the energy $hc\tilde{\nu}_{flu}$ and the solvent polarity function in a polar environment and also in all the solvents including alkanes (Figure 6). The fit can not be improved by taking into account the solute polarizability effects.[51,53]

The experiments allow us to estimate the values of $\vec{\mu}_e(\vec{\mu}_e - \vec{\mu}_g)/a_o^3$ and $\tilde{\nu}_{flu}^{vac}$; the results are collected in Table 1. It should be noted, however, that these values, extracted from the data measured in polar media, are somewhat larger than those resulting from the analysis of the data obtained for the whole range of the solvents. The effect increases with the energy of the emitting state as well as with the interactions between A and D subunits (as expressed in terms of an electronic transition dipole moment *M*, cf. Tables 4 and 5 and eq 18). This finding can be explained by the dependence of the electronic structure of the fluorescent states on solvation. Due to a relatively small energy gap between the lowest ^{1}CT states and the states excited locally in the donor (and acceptor?) subunit in nonpolar solvents, one can expect an increase of the contribution of the $^1(\pi,\pi^*)$ character to the wave function of the CT states. It leads to a lowering of energy with respect to a "pure" CT state because of a stabilizing character of such interactions.

TABLE 2: Results of the CT Band-Shape Analysis within a Semiclassical Description Including a Single High-Frequency Mode Approximation Using Eq 4 (λ_i and $h\nu_i$) or Eqs 4 and 7 ($\delta\lambda_o$ and $(\vec{\mu}_e - \vec{\mu}_g)^2/a_o^3$)

compound	λ_i, eV	$h\nu_i$, eV	$\delta\lambda_o$, eV	$(\vec{\mu}_e - \vec{\mu}_g)^2/a_o^3$, eV
CNO	0.31	0.17	0.11	0.97
CBO	0.21	0.19	0.07	1.21
CPO	0.22	0.18	0.09	1.25
CTO	0.22	0.19	0.11	1.34
CIP	0.18	0.19	0.10	1.25
CBM	0.22	0.18	0.09	1.56
CBP	0.21	0.19	0.08	1.68
CNP	0.21	0.19	0.17	1.47
CIM	0.25	0.16	0.11	1.40
CPM	0.18	0.20	0.13	1.54

Under the assumption that the CT fluorescence corresponds to the state reached directly upon excitation, the quantity $(\vec{\mu}_e - \vec{\mu}_g)^2/a_o^3$ can be evaluated from the solvation effects on the Stokes shift[49,51]

$$hc(\tilde{\nu}_{abs} - \tilde{\nu}_{flu}) = hc(\tilde{\nu}_{abs}^{vac} - \tilde{\nu}_{flu}^{vac}) + \frac{2(\vec{\mu}_e - \vec{\mu}_g)^2}{a_o^3}\left[\frac{\epsilon - 1}{2\epsilon + 1} - \frac{n^2 - 1}{2n^2 + 1}\right] \quad (3)$$

Considering the limitations of the model (as shown by the solvent effects on the absorption spectra), the corresponding values of $(\vec{\mu}_e - \vec{\mu}_g)^2/a_o^3$, estimated for the compounds showing a distinctly separated CT absorption band (CTO, CIP and CPM), are similar to those of $\vec{\mu}_e(\vec{\mu}_e - \vec{\mu}_g)/a_o^3$ resulting from the analysis of the solvatochromic effects on the fluorescence spectra.

The eqs 1−3 relate the measured quantities to the excited state dipole moments $\vec{\mu}_e$. Under the assumption that $|\vec{\mu}_e| \gg |\vec{\mu}_g|$ and with the effective spherical radius of the D−A molecules $a_o \approx 0.6$ nm (as estimated[48] from the molecular dimensions of the compounds calculated by molecular mechanics), eqs 2 and 3 yield very similar values of $\vec{\mu}_e$ being in the range of 19−21 D and 22−24 D for the molecules with and without a cyano group in the ortho position with respect to the D−A bond, respectively. Such large values correspond to a CT distance of about 0.40−0.45 nm, which roughly agrees with the center-to-center distance between the donor and acceptor moieties of the compounds and suggest that the full (or nearly full) electron transfer takes place in all the D−A systems studied.

This conclusion is in agreement with a linear relationship found between the CT fluorescence energies and the differences in the redox potentials corresponding to the oxidation of the donor subunit E_{ox}(D) and the reduction of the acceptor moiety E_{red}(A) in the D−A molecules. The correlation is shown in Figure 7, where the results obtained for the carbazole derivatives are compared with the data reported previously[54] for aryl derivatives of *N*,*N*-dimethylaniline.

In this correlation the values of E_{ox}(D)−E_{red}(A) are taken from the electrochemical data obtained for the given D−A molecule in ACN containing 0.1 M $TBAPF_6$. These values, however, are very similar to those expected from the electrochemical properties of the donor and acceptor alone; the standard oxidation potentials E_{ox}(D), as well as the standard reduction potentials E_{red}(A), were close to the values found for CAR[55] and a proper acceptor,[56] respectively. The small shift of E_{red}(A) to more negative potentials can be explained by the electron donating properties of 3,6-di-*tert*-butylcarbazole bonded to the acceptor subunit. Correspondingly, the small shift of E_{red}(D) to more positive potentials arises from the electron withdrawing character of the acceptor moiety. The E_{red}(A) and E_{ox}(D) values indicate also (in agreement with the absorption spectra) that both subunits of all the D−A molecules studied interact very weakly.

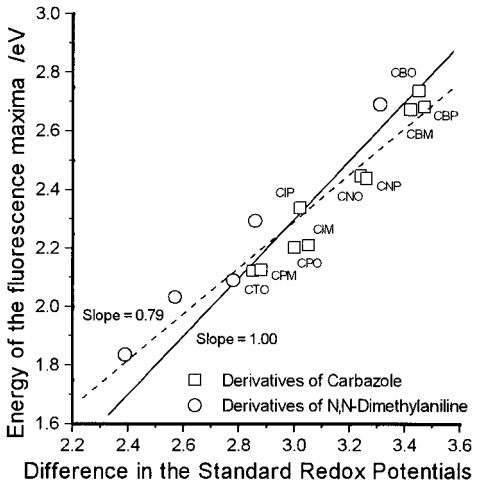

Figure 7. Correlation between the energy of the fluorescence maxima of the D−A derivatives of carbazole (squares) and aryl derivatives of *N*,*N*-dimethylaniline[54] (circles) in acetonitrile at room temperature and the difference in the standard redox potentials. The best fit corresponds to a slope of 0.79, the line with the "theoretical" slope of 1.00 is presented for the comparison.

3.2. CT Band-Shape Analysis. Pursuing the analogy between CT optical spectroscopy and thermal electron transfer processes, as has been shown by Marcus,[57] the following expression for the CT fluorescence profile can be derived[57−59]

$$\frac{I(\tilde{\nu}_f)}{n^3\tilde{\nu}_f^3} = \frac{64\pi^4}{3h}M^2\sum_{j=1}^{\infty}\frac{e^{-S}S^j}{j!} \times \sqrt{\frac{1}{4\pi\lambda_o k_B T}}\exp\left[-\frac{(jh\nu_i + \lambda_o + hc\tilde{\nu}_f + \Delta G_{CT})^2}{4\lambda_o RT}\right] \quad (4)$$

with S being the electron-vibration coupling constant

$$S = \lambda_i/h\nu_i \quad (5)$$

and where M is the electronic transition dipole moment; $\tilde{\nu}_f$, the wavenumber of the emission ($hc\tilde{\nu}_f$ is the energy of the emitted photon); ΔG_{CT} is the free energy of the charge recombination process, k_B, the Boltzmann constant; and T, the temperature. The inner reorganization energy λ_i corresponds to the high-frequency motions (represented by a single "averaged" mode characterized by ν_i) associated with the changes in the solute bond lengths and angles. The reorganization energy λ_o is related to the low-frequency motions such as reorientation of the solvent shell (λ_s) as well as any other low- and medium-frequency nuclear motions of the solute ($\delta\lambda_o$) undergoing electron transfer. Following the procedure of the band-shape analysis of the CT fluorescence spectra proposed by Cortes, Heitele, and Jortner,[59] the quantities relevant for the electron transfer (i.e., ΔG_{CT}, $h\nu_i$, λ_i, and λ_o) were varied as free fit parameters. It has been done with an assumption that the electronic transition dipole moment value M is independent of the emitted (absorbed) photon energy. It seems to be justified in view of the results of the excited CT state depopulation kinetics (Tables 3 and 4). It should be stressed that nearly the same results are obtained in the analysis taking into account the dependence of M vs $\tilde{\nu}_f$ (cf. also ref 59). Representative examples of the numerical fits (within a single

TABLE 3: Solvent Effects on the Spectral Position of the Fluorescence Maxima ($\tilde{\nu}_{flu}$), Quantum Yields (Φ_f), Decay Times (τ) and Resulting Radiationless (k_{nr}) and Radiative (k_f) Rate Constants, and Electronic Transition Dipole Moments (M) of CBO, CBM, CBP, CNO, and CNP at Room Temperature

compound	solvent	$\tilde{\nu}_{flu}$[a], cm^{-1}	Φ_f[b]	τ[b], ns	k_{nr}, $10^7\ s^{-1}$	k_f, $10^7\ s^{-1}$	M, D
CBO	HEX	26 400	0.12	3.5	25.1	3.4	1.5
	BE	24 900	0.16	9.1	9.2	1.8	1.2
	THF	23 475	0.26	15.4	4.8	1.7	1.2
	ACN	22 075	0.30	36.0	1.9	0.83	1.0
CBM	HEX	27 550	0.11	6.5	13.7	1.7	1.0
	BE	25 550	0.14	11.0	7.9	1.2	0.9
	THF	23 625	0.25	22.5	3.3	1.1	1.0
	ACN	21 525	0.31	56.0	1.2	0.55	0.9
CBP	HEX	27 600	0.35	4.9	13.3	7.1	2.0
	BE	25 750	0.31	6.4	10.8	4.8	1.8
	THF	23 700	0.33	7.9	8.5	4.2	1.9
	ACN	21 625	0.41	17.7	3.4	2.3	1.7
CNO	HEX	23 625	0.11	11.8	7.6	0.88	0.9
	BE	22 450	0.11	14.3	6.3	0.73	0.9
	THF	21 050	0.25	27.6	2.7	0.91	1.1
	ACN	19 700	0.12	24.1	3.7	0.50	0.9
CNP	HEX	25 150	0.46	5.9	59.2	7.6	2.4
	BE	23 575	0.35	7.4	8.8	4.7	2.0
	THF	21 575	0.36	11.9	5.4	3.0	1.9
	ACN	19 700	0.29	13.3	5.4	2.2	2.0

[a] Scatter of results is ±100−150 cm^{-1}. [b] Error is about 10%. Thus the maximum error is about 20% for the rate constants k_f and k_{nr} and about 10% for the transition moment M.

TABLE 4: Solvent Effects on the Spectral Position of the Fluorescence Maxima ($\tilde{\nu}_{flu}$), Quantum Yields (Φ_f), Decay Times (τ) and Resulting Radiationless (k_{nr}) and Radiative (k_f) Rate Constants, and Electronic Transition Dipole Moments (M) of CIM, CIP, CPO, CPM, and CTO at Room Temperature

compound	solvent	$\tilde{\nu}_{flu}$[a], cm^{-1}	Φ_f[b]	τ[b], ns	k_{nr}, $10^7\ s^{-1}$	k_f, $10^7\ s^{-1}$	M, D
CIM	HEX	23 150	0.067	12.7	7.3	0.53	0.7
	BE	21 575	0.12	29.6	3.0	0.40	0.7
	THF	19 550	0.24	42.9	1.8	0.56	0.9
	ACN	17 825	0.055	19.3	4.9	0.28	0.8
CIP	HEX	23 300	0.29	13.9	5.1	2.1	1.4
	BE	21 850	0.23	17.0	4.5	1.4	1.3
	THF	20 175	0.61	22.4	1.7	2.7	1.9
	ACN	18 850	0.30	19.0	3.7	1.6	1.8
CPO	HEX	23 125	0.16	14.3	5.9	1.1	1.0
	BE	20 925	0.19	32.7	2.5	0.58	0.9
	THF	19 300	0.33	46.2	1.5	0.71	1.1
	ACN	17 650	0.02	7.6	12.9	0.26	0.8
CPM	HEX	23 975	0.38	12.2	5.1	3.1	1.7
	BE	21 650	0.38	17.8	3.5	2.1	1.6
	THF	19 450	0.47	21.5	2.5	2.2	1.8
	ACN	17 200	0.05	4.8	19.9	1.0	1.6
CTO	HEX	22 325	0.31	26.3	2.6	1.2	1.2
	BE	20 175	0.255	35.0	2.1	0.73	1.0
	THF	18 450	0.17	23.6	3.5	0.72	1.2
	ACN	17 125	0.017	4.7	20.9	0.36	1.0

[a] Scatter of results: ±100−150 cm^{-1}. [b] Error is about 10%. Thus the maximum error is about 20% for the rate constants k_f and k_{nr} and about 10% for the transition moment M.

high-frequency mode approximation according to eq 4) of the CT fluorescence spectra are presented in Figure 8; the experimental emission profiles of all the D−A compounds studied in the whole range of the solvents could be adequately reproduced. It should be noted, however, that ΔG_{CT} and λ_o as well as $h\nu_i$ and λ_i turn out to be somewhat correlated, leading to a numerical uncertainty (standard deviations) of their values of about ±0.02 eV (because of the model approximations the real uncertainty can be somewhat larger).

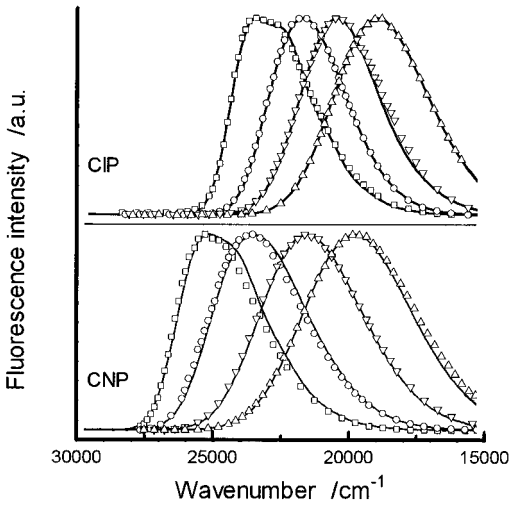

Figure 8. Room temperature CT fluorescence spectra of CNP and CIP in *n*-hexane, butyl ether, tetrahydrofuran, and acetonitrile (from left to right, respectively) and the corresponding numerical fits (solid lines) using eq 4.

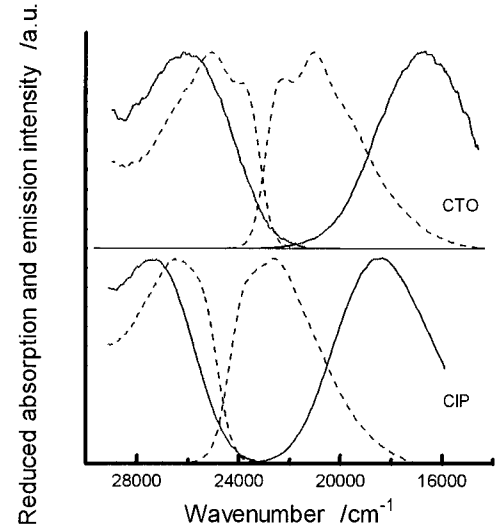

Figure 9. Room temperature reduced and normalized CT absorption and CT fluorescence spectra (see text) for CIP and CTO in *n*-hexane (dotted lines) and acetonitrile (solid lines).

In a similar way, the molar absorption coefficient $\epsilon(\tilde{\nu}_a)$ for CT absorption of a given photon with the energy $hc\tilde{\nu}_a$ can be expressed as follows:[57]

$$\frac{\epsilon(\tilde{\nu}_a)}{n\tilde{\nu}_a} = \frac{8\pi^3}{3\ln 10}\frac{M^2}{c}\sum_{j=1}^{\infty}\frac{e^{-S}S^j}{j!} \times \sqrt{\frac{1}{4\pi\lambda_o k_B T}}\exp\left[-\frac{(jh\nu_i + \lambda_o - hc\tilde{\nu}_a + \Delta G_{CT})^2}{4\lambda_o RT}\right] \quad (6)$$

Figure 9 shows the comparison of the reduced CT absorption bands (as plotted in the form $\epsilon(\tilde{\nu})/\tilde{\nu}$ vs $\tilde{\nu}$) and the CT emission spectra (i.e., a plot of the normalized reduced intensity $I(\tilde{\nu})/\tilde{\nu}^3$ vs $\tilde{\nu}$) of CTO and CIP in a nonpolar (HEX) and polar (ACN) environment; the corresponding spectra exhibit a mirror relationship. Consequently, the CT absorption bands are reproducible with the same set of the energetic and nuclear parameters as obtained from the analysis of the respective CT emission profiles.

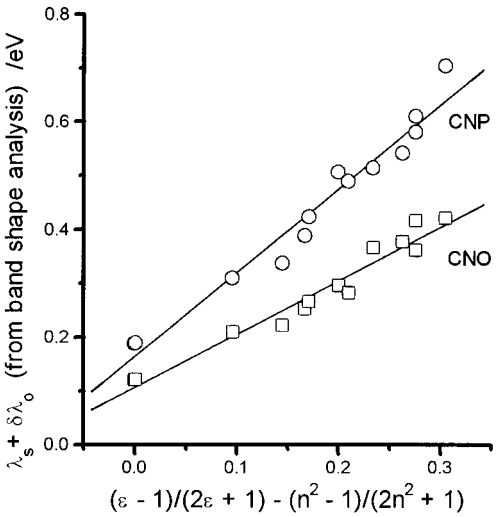

Figure 10. Correlation between the reorganization energy λ_o and the solvent polarity function corresponding to eq 7.

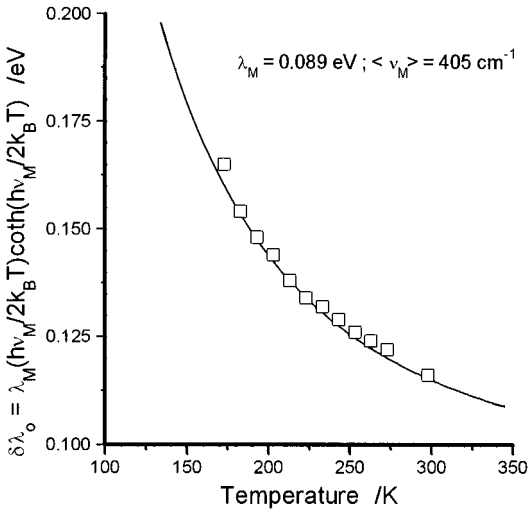

Figure 11. Fit (solid line) of the dependence of the reorganization energy $\delta\lambda_o$ (obtained from eq 4, squares) on temperature in the semiclassical approximation according to eq 8 for CTO in methylcyclohexane. The intermediate wavenumber $\tilde{\nu}_M \approx 400$ cm^{-1} of the intramolecular vibration mode and the corresponding value of the reorganization energy $\lambda_M \cong 0.089$ eV result from the analysis where both quantities were varied as free fit parameters (see text).

For the given D−A molecule, the quantities λ_i and $h\nu_i$ (collected in Table 2) have been found to be nearly constant (with uncertainty of about ±0.02 eV) over the whole solvents range. The $h\nu_i$ values (being about 0.16−0.20 eV) seem to correspond to the stretching vibrations of the C−C and C−N bonds.[60] The values of λ_i are in a reasonable agreement with the results of AM1 semiempirical calculations. The difference between the computed values of the heat of formation of the donor in its equilibrium nuclear geometry and in the conformation corresponding to the equilibrium geometry of its radical cation is added to the respective value calculated for the acceptor and its radical anion. The sum of these energy differences can be regarded as a lower limit of the inner reorganization energies. The calculated values (being in the range of 0.17−0.19 eV) are somewhat smaller than those obtained experimentally (Table 2), but the above approach neglects the changes of the nitrogen−carbon bond between the donor and acceptor subunits.

The values of ΔG_{CT} and λ_o extracted from the band-shape analysis depend on the solvent polarity, as expected. The more polar is the medium, the smaller is the energy gap between the ground and excited CT states and the larger is the outer reorganization energy λ_s, in agreement with the continuum dielectric model of solvation. An analysis of the solvent effects on λ_o is possible according to eq 7[28,61]

$$\lambda_o \cong \delta\lambda_o + \lambda_s = \delta\lambda_o + \frac{(\vec{\mu}_e - \vec{\mu}_g)^2}{a_o^3}\left[\frac{\epsilon - 1}{2\epsilon + 1} - \frac{n^2 - 1}{2n^2 + 1}\right] \quad (7)$$

This relation is different from the classical Marcus expression,[62] but it is more suitable for the direct comparison with the results of the investigations of the solvatochromic effects on the spectral position of the CT fluorescence maxima and the Stokes shift (eqs 2 and 3). Typical dependence of the reorganization energy λ_o on the solvent polarity function is presented in Figure 10. The values of $(\vec{\mu}_e - \vec{\mu}_g)^2/a_o^3$ obtained from the slopes of the plots corresponding to eq 7 (Table 2) agree well with those collected in Table 1 and confirm again that $|\vec{\mu}_e| \gg |\vec{\mu}_g|$.

The values of $\delta\lambda_o$ estimated from the intercepts of the plot of λ_o vs solvent polarity function (eq 7) are in the range of 0.07−0.13 eV for all the D−A carbazole derivatives excluding CNP (Table 2). As mentioned above, $\delta\lambda_o$ can be connected with the low-frequency intramolecular vibration mode ($\nu_L <$ 200 cm^{-1}, e.g., associated with librations, internal rotations) with a reorganization energy λ_L and with the medium-frequency mode of the solute ($\tilde{\nu}_M \cong 300-600$ cm^{-1}) with a reorganization energy λ_M.[59] Information about the relative contributions of λ_L and λ_M to $\delta\lambda_o$ can be obtained from the analysis of the temperature effects on the CT fluorescence spectra. In our case the experiments were performed in a nonpolar solvent (MCH) to minimize possible effects caused by the temperature dependence of the solvent properties (ϵ and n). The quantities ΔG_{CT}, $h\nu_i$, λ_i, and λ_o were again varied as free fit parameters. Within uncertainty limits of our analysis, the values obtained for $h\nu_i$ and λ_i were again constant; the variations of the CT emission profile are mainly due to the changes of λ_o (i.e., $\delta\lambda_o$, because in MCH $\epsilon = n^2$). It has been found that the effective $\delta\lambda_o$ values increase with a lowering of the temperature (Figure 11).

To analyze this effect, all the low- and medium-frequency parameters λ_L, λ_M, and ν_M were explicitly included in fitting the temperature dependence of $\delta\lambda_o$. The dependence of the band shapes on the frequency ν of the emitted (or absorbed) photon remains the same as in the single high-frequency mode description. The most important difference is connected with the denominator in the exponential part of eqs 4 and 6

$$4\lambda_o k_B T = 4k_B T\left[\lambda_s + \lambda_L + \lambda_M \frac{h\nu_M}{2k_B T}\coth\left[\frac{h\nu_M}{2k_B T}\right]\right] \quad (8)$$

It should be stressed that the procedure of the analysis was somewhat different than that proposed in ref 59; three quantities ($\lambda_s + \lambda_L$), λ_M, and ν_M were varied as free fit parameters. Fitting the data of the temperature dependence of $\delta\lambda_o$ shows that the sum ($\lambda_s + \lambda_L$) in eq 8 is negligible; on the contrary, a contribution of the medium-frequency intramolecular mode is important (e.g., for CTO with the wavenumber $\tilde{\nu}_M \approx 400$ cm^{-1} and the reorganization energy $\lambda_M \approx 0.09$ eV). It suggests that the intramolecular nuclear motions of the D−A carbazole derivatives coupled to the electron transfer are not connected with a torsion around the single D−A bond; $\tilde{\nu}_M \approx 400$ cm^{-1} corresponds most probably to a ring skeletal vibration.[60]

It should be noted that the modification of the denominator in the exponential part of eqs 4 and 6 as expressed by eq 8 requires a simple reinterpretation[59] of the quantities ΔG_{CT} and λ_o fitted according to eqs 4 and 6

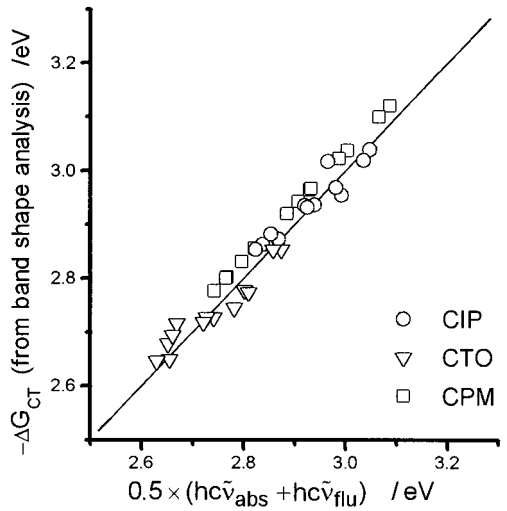

Figure 12. Correlation between the free energy of the charge recombination process ΔG_{CT} obtained from the CT fluorescence band-shape analysis in a single high-frequency mode approximation according to eq 4 and the sum of the energies corresponding to the maxima of the reduced CT absorption and fluorescence spectra (eq 13) for CIP, CTO, and CPM in the whole range of the solvents used.

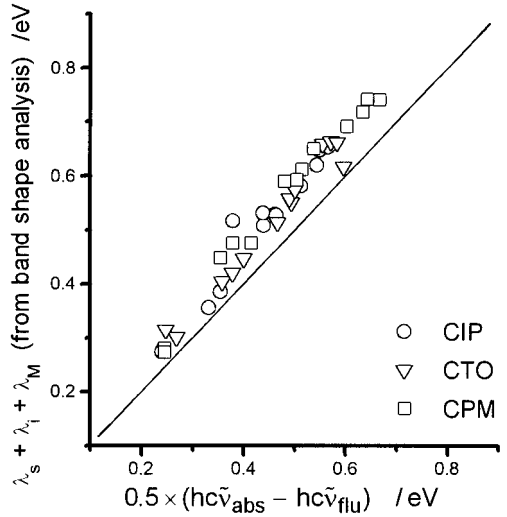

Figure 13. Correlation between the sum of the reorganization energies and the energy corresponding to the Stokes shift between the reduced CT absorption and fluorescence maxima (eq 14) for CIP, CTO, and CPM in the whole range of the solvents used.

$$\lambda_o(\text{true}) = \lambda_o(\text{fit}) - \delta\lambda_o\left[1 - \frac{2k_BT}{h\nu_M}\tanh\left[\frac{h\nu_M}{2k_BT}\right]\right] \quad (9)$$

$$\Delta G_{CT}(\text{true}) = \Delta G_{CT}(\text{fit}) + \delta\lambda_o\left[1 - \frac{2k_BT}{h\nu_M}\tanh\left[\frac{h\nu_M}{2k_BT}\right]\right] \quad (10)$$

The above corrections to ΔG_{CT} and λ_o, however, are small (being smaller than 0.05 eV at room temperature).

From eqs 4 and 6 modified by relation 8 the following approximate expressions for the CT absorption and fluorescence maxima can be derived:

$$hc\tilde{\nu}_{abs} \approx -\Delta G_{CT} + \lambda_s + \lambda_i + \lambda_M \quad (11)$$

$$hc\tilde{\nu}_{flu} \approx -\Delta G_{CT} - \lambda_s - \lambda_i - \lambda_M \quad (12)$$

allowing an independent verification of the computed data. The absorption and fluorescence maxima are simply connected with ΔG_{CT}

$$-\Delta G_{CT} \approx \frac{1}{2}(hc\tilde{\nu}_{abs} + hc\tilde{\nu}_{flu}) \quad (13)$$

and, correspondingly, their difference with the sum of all the reorganization energies

$$hc\tilde{\nu}_{abs} - hc\tilde{\nu}_{flu} \approx 2(\lambda_s + \lambda_i + \lambda_M) \quad (14)$$

The experimental positions of the CT absorption and fluorescence maxima as well as the values of Stokes shift agree well (cf. Figures 12 and 13) with those predicted by the band-shape analysis. The sums $\lambda_s + \lambda_i + \lambda_M$, however, are slightly larger (about 0.05 eV) than the experimental Stokes shift. The observed deviations can be hardly rationalized, because they are within the accuracy of the fitting procedures (ca. 3 × 0.02 eV).

3.3. Excited CT State Depopulation Kinetics. Applying a simple kinetic model of an irreversible excited charge transfer state formation (with 100% efficiency) the radiationless (k_{nr}) and radiative (k_f) rate constants can be determined from the CT fluorescence quantum yields Φ_f and lifetimes τ

$$k_{nr} = (1 - \Phi_f)/\tau \quad (15)$$

and

$$k_f = \Phi_f/\tau \quad (16)$$

The experimental k_f and k_{nr} values for all the D−A carbazole derivatives in selected solvents are collected in Tables 3 and 4. The radiative rate constants allow us to obtain the electronic transition dipole moments M[63]

$$k_f = \frac{64\pi^4}{3h}n^3\tilde{\nu}_{flu}^3|M|^2 \quad (17)$$

The electronic transition dipole moment M is mainly determined by the direct interactions between the lowest ^{1}CT state and the ground state and by the contribution from locally excited (LE) configurations[64]

$$M = \frac{V_{AD}(\vec{\mu}_e - \vec{\mu}_g)}{hc\tilde{\nu}_{flu}} + \sum_i \frac{V_iM_i}{E_i - hc\tilde{\nu}_{flu}} \quad (18)$$

where V_{AD} and V_i are the electronic coupling elements between the ^{1}CT state and the ground state or between the ^{1}CT state and ^{1}LE states "i" of energy E_i, respectively, and M_i is an electronic transition moment corresponding to the radiative transition $(^1\text{LE})_i \rightarrow S_o$. The important result is that the values of M do not show any clear dependence on the solvent polarity (Tables 3 and 4). Contrary to aryl derivatives of aromatic amines,[27,28] the electronic transition dipole moments for CIM and CIP increase with solvent polarity; the M values for the other D−A carbazole derivatives are roughly constant in polar solvents ranging from BE to ACN. The lack of any significant lowering of the M values with increasing energy gap between the emitting ^{1}CT state and ^{1}LE states in highly polar media strongly suggests that the first term in eq 18 is dominant in the description of the radiative properties of the compounds studied.[64] This hypothesis is confirmed by the analysis of the absorption spectra (Figures 2 and 3); no spectral evidence of the significant role of the mechanism expressed by the second term in eq 18 is observed. For example, the dramatic increase of the intensity of the first absorption band in CBP and CNP with respect to that of CAR or the appearance of the intense CT band in CPM and CIP do not generate any marked decrease

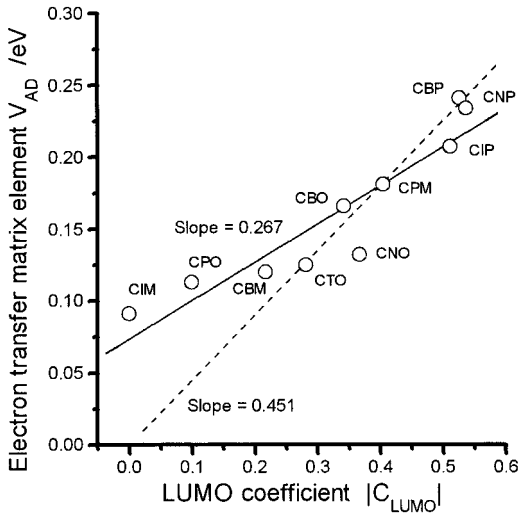

Figure 14. Correlation between the electronic coupling elements V_{AD} between the ^{1}CT state and the ground state (as estimated from the experimental electronic transition dipole moments M under the assumption that the first term in eq 18 plays a dominant role in the description of the radiative properties of the lowest ^{1}CT states of all the D−A carbazole derivatives in acetonitrile) and the absolute values of the LCAO coefficients of the LUMO orbital at the carbon atom of the donor−acceptor bond (as calculated by AM1 method, see Table 6).

of the intensity of the bands corresponding to the donor and acceptor subunits. The dependence of the experimental values of M on $\tilde{\nu}_{flu}$ is smaller than that expected from the first term of eq 18; most probably it is due to small contributions connected with the mixing of the ^{1}CT state and ^{1}LE states.

The values of the electronic coupling element V_{AD} (as estimated from the experimental M values under the assumption that the direct interactions between the lowest ^{1}CT state and the ground state (first term in eq 18) play a dominant role in the description of the radiative properties of the lowest ^{1}CT states of all the D−A carbazole derivatives in ACN) are found to be correlated with the absolute values of the LCAO coefficient of the acceptor LUMO orbital at the carbon atom of the donor−acceptor bond (Figure 14).

Following Dogonadze et al.,[65] the electronic coupling element V_{AD} between the ^{1}CT state and the ground state can be related to the sum of the products of the LCAO coefficients of the highest occupied molecular orbital (HOMO) at an atom in the donor moiety and of the lowest unoccupied molecular orbital (LUMO) at another atom in the acceptor subunit and the corresponding resonance integrals $\beta_{ad}(r_{ad}, \varphi_{ad})$ for the given pair of atoms

$$V_{AD} = \sum_{a=1}^{n}\sum_{d=1}^{m} C_{LUMO}(a) C_{HOMO}(d) \beta_{ad}(r_{ad}, \varphi_{ad}) \qquad (19)$$

By assuming that V_{AD} is mainly determined by the interactions between the carbon and nitrogen atoms forming A−D bond (which is reasonable because the resonance integral β_{ad} is an exponential function of a distance) and by neglecting contributions from the σ orbitals, the above relationship can be simplified

$$V_{AD} = C_{LUMO} C_{HOMO} \beta_{CN} \cos(\Theta_{A-D}) + \text{const} \qquad (20)$$

where Θ_{A-D} is the angle between the planes of the donor and acceptor subunits and C_{LUMO} and C_{HOMO} are the corresponding LCAO coefficients of the $2p_z$ atomic orbitals (where z is the axis perpendicular to the acceptor ring) of the carbon and nitrogen atoms forming A−D bond, respectively. The values

TABLE 5: Results of Semiempirical AM1 and Molecular Mechanics Calculations: $|\vec{\mu}_g|$, Ground State Dipole Moments; Θ_{A-D}, Angles between the Planes of the Donor and Acceptor Subunits; and C_{LUMO}, LCAO Coefficients of the $2p_z$ Atomic Orbital at the Carbon Atom in the Donor−Acceptor Bond

compound	AM1, $\|\vec{\mu}_g\|$ D	MMX,[a] D	AM1, Θ_{A-D} deg	MMX,[b] deg	$\|C_{LUMO}\|$ AM1	$\|C_{LUMO}\|$ ESR[c]
CBM	3.0	4.7	44	53	0.217	0.109
CBO	3.5	4.3	51	64	0.342	0.381
CBP	2.9	4.3	41	54	0.526	0.580
CNO	3.3	3.8	50	49	0.367	
CNP	2.6	3.7	40	38	0.537	
CIP	3.5	4.3	48	61	0.512	0.576
CIM	2.9	4.3	43	53	0.000	0.050
CPM	5.2	7.0	41	53	0.405	0.406
CPO	5.1	7.0	51	62	0.100	0.130
CTO	0.7	0.3	53	64	0.282	0.252

[a] Experimental values of the ground state dipole moments for the acceptors:[69,70] Benzonitrile, 4.0 D; nicotinonitrile, 3.5 D; isophthalonitrile, 4.1 D; phthalonitrile, 6.2 D; and terephthalonitrile, 0.0 D. The corresponding value for carbazole is 1.7 D.[71] [b] X-ray crystallographic data[72] for *N*-phenylcarbazole and *N*-(2-pyridyl)carbazole indicate a presence of two conformers, with the following torsion angles between carbazole and phenyl (78.4 and 54.8°) or pyridyl (61.9 and 47.6°) rings. The AM1 values[72] are 48 and 38°, respectively. [c] As estimated from the experimental proton hyperfine spliting constants a_H of the ESR spectra of the acceptor anion radicals[67] using McConnell relationship:[66] $a_H = Q_{CH}(C_{LUMO})^2$ with $Q_{CH} = 25$ G.

C_{LUMO} and C_{HOMO} can be obtained in two independent ways: (i) from semiempirical AM1 calculations and (ii) from the hyperfine structure of the ESR spectra[66] of the respective radical anions[67] and cations.[68] Both methods yield very similar values (Table 5). Similarly, one can describe the electronic coupling elements V_i between the ^{1}CT state and ^{1}LE states either connected with the donor (by taking into considerations the LCAO coefficients of the LUMO (and higher UMO) orbitals at respective pair of atoms in the donor and acceptor subunits) or with the acceptor (the HOMO (and lower OMO) orbitals should be considered). The large value (0.503) of the LCAO coefficient of the HOMO orbital at the carbazole nitrogen atom and the small ones (0.153 and 0.00) of the corresponding coefficients of the LUMO and LUMO + 1 orbitals, respectively, agree well with the dominant role of the interactions between the emitting charge transfer ^{1}CT state and the ground state.

The slope of the plot of the relation between V_{AD} and C_{LUMO} (eq 20) allows us to estimate qualitatively the angle Θ_{A-D}. The values 65° (slope = 0.451 and const = 0) and 75° (slope = 0.265 and const > 0) can be regarded as the lower and upper limits. The range of the Θ_{A-D} values (calculated with β_{CN} = 2 eV) agree well with the crystallographic data available for *N*-pyridyl- and *N*-phenylcarbazoles.[72] The intercept value higher than zero can arise from two reasons: (i) the not negligible interactions between the pairs of atoms different than those forming the A−D bond, and/or (ii) the values of the LCAO coefficients of $2p_z$ orbitals can be somewhat affected by the interacting positive and negative charges in the contact ion pair forming the excited CT state.

It should be pointed out, however, that for all the D−A carbazole derivatives in nonpolar solvents (HEX, MCH) the electronic coupling elements V_{AD} estimated from the experimental M values under the assumption that the first term in eq 18 plays a dominant role in the description of the radiative properties of the fluorescent ^{1}CT states are slightly larger than those predicted from the correlation observed in a polar environment and shown in Figure 14. It suggests strongly that due to a decreasing energy gap between these states the

contribution of the LE configurations to M is not negligible in nonpolar media. Similarly as for V_{AD} values, the difference between the calculated values of V_{AD}(HEX) and V_{AD}(ACN) (eq 18) increases in line with the LCAO coefficient of the acceptor LUMO orbital at the carbon atom of the D−A bond. It suggests that the respective V_i values can be also discussed in terms of the expression similar to eq 20. The lack of the fluorescence data in solvents with dielectric constants between 2 and 3 does not allow us for a more quantitative discussion, but the V_i values seem to be small with respect to those of V_{AD}.

Similar correlation between M and C_{LUMO} is observed for absorption, but too small energy gaps between the corresponding Franck−Condon CT and LE states do not permit the discussion in terms of respectively modified eq 18.

The nonradiative depopulation of the lowest excited ^{1}CT state of the studied compounds, similarly to aryl derivatives of aromatic amines,[27] is most probably controlled by two competitive mechanisms—the intersystem crossing (ISC) to the triplet manifold and a direct radiationless charge recombination (DICR) process in the singlet manifold. To examine the latter process it should be recognized to what degree the nonradiative deactivation of the ^{1}CT state can be assigned to the DICR path and how far to the ISC processes (generally, ISC may occur to the charge transfer ^{3}CT triplet state and/or to the locally excited $^3(\pi,\pi^*)$ triplet states). The efficiency of the radiationless depopulation path via the triplet manifold in various D−A systems should depend on the energy of the $^3(\pi,\pi^*)$ states with respect to that of the ^{1,3}CT states. The comparative investigations of the lowest excited triplet states T_1 in the series of D−A carbazole derivatives undoubtedly show the change of their electronic structure with the increasing electron affinity of the acceptor moiety.[73] (3,6-Di-*tert*-butylcarbazol-9-yl)benzonitriles and (3,6-di-*tert*-butylcarbazol-9-yl)nicotinonitriles exhibit a number of phosphorescence features characteristic of carbazole (the energy of the lowest triplet state localized on the donor moiety is about 3 eV), and the ESR measurements clearly indicate that the spin density in the emitting T_1 state is mainly distributed over the carbazole π-system. These results point unambiguously to the dominant $^3(\pi,\pi^*)$ character of the lowest triplet states, the excitation being mainly localized in the donor moiety. On the contrary, the solvent, concentration, and temperature effects on the long-lived emission (phosphorescence and delayed fluorescence), measurements of low-temperature luminescence polarization and lifetimes, and ESR investigations do point to a CT character of the emitting T_1 states of (3,6-di-*tert*-butylcarbazol-9-yl)dicyanobenzenes.[73]

The dependence of the nonradiative rate constants k_{nr} on the spectral positions of the CT fluorescence maxima at room temperature for all the D−A carbazole derivatives suggests that ISC is the dominant radiationless deactivation path for the D−A systems with $\tilde{\nu}_{flu} \geq 20\,000$ cm^{-1} (Table 6 and Figure 15). The decrease of the energy gap between the excited ^{1}CT state and the ground state ($\tilde{\nu}_{flu} < 20\,000$ cm^{-1}) induces the increase of the rate of the direct CR process (the similar effect is observed for aryl derivatives of aromatic amines[27]).

Experimental rate constants of the DICR (k_{nr} values in highly polar solvents like ACN, DMSO, and DMF) can be compared with those calculated from the following relation:[74]

$$k_{nr} = \frac{4\pi^2}{h} V_{AD}^2 \sum_{j=1}^{\infty} \frac{e^{-S} S^j}{j!} \times \sqrt{\frac{1}{4\pi\lambda_o k_B T}} \exp\left[-\frac{(jh\nu_i + \lambda_o + \Delta G_{CT})^2}{4\lambda_o RT} \right] \quad (21)$$

TABLE 6: Comparison between Experimental (Eq 15) and Computed (Eq 21) k_{nr} Values (Data in Acetonitrile Solutions)

compound	λ_i, eV	$h\nu_i$, eV	λ_o, eV	$-\Delta G_{CT}$[a], eV	V_{AD}, eV	k_{nr}(calcd), 10^7 s^{-1}	k_{nr}(exptl), 10^7 s^{-1}
CBM	0.22	0.18	0.55	3.30	0.12	0.008	1.2
CBO	0.21	0.19	0.47	3.25	0.17	0.008	1.9
CBP	0.21	0.19	0.61	3.35	0.24	0.07	3.4
CNO	0.31	0.17	0.42	3.05	0.13	1.1	3.7
CNP	0.21	0.19	0.71	3.23	0.23	1.5	5.4
CIP	0.18	0.19	0.51	2.92	0.21	0.4	3.7
CIM	0.25	0.16	0.53	2.85	0.09	1.1	4.9
CPM	0.18	0.20	0.61	2.80	0.18	14.1	19.9
CPO	0.22	0.18	0.47	2.76	0.11	1.9	12.9
CTO	0.22	0.19	0.48	2.72	0.13	10.0	20.9

[a] Energy of the lowest $^3(\pi,\pi^*)$ triplet state localized on the donor moiety is about 3.0 eV. Thus, contrary to the benzonitrile derivatives (CBM, CBO, and CBP), the nearly degenerated charge transfer states (^{1}CT and ^{3}CT) of all dicyanobenzene derivatives (CIP, CIM, CPM, CPO, and CTO) are lying energetically lower than the former one[73] (the nicotinonitrile derivatives (CNO and CNP) seems to be a border case).

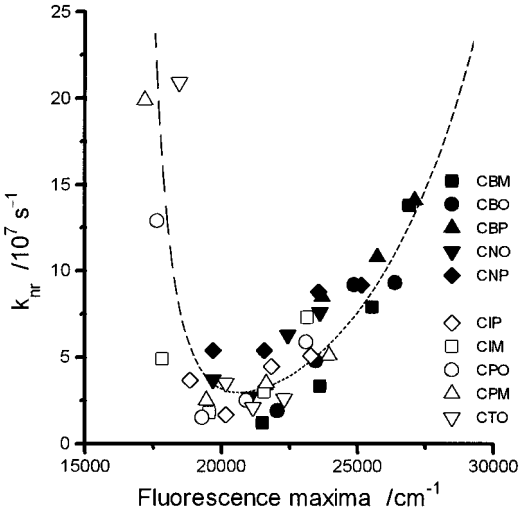

Figure 15. Dependence of the radiationless rate constants k_{nr} on the spectral position of the CT fluorescence maxima at room temperature for all the D−A carbazole derivatives in selected solvents (*n*-hexane, butyl ether, tetrahydrofuran, and acetonitrile). An arbitrary dashed line is drawn to show the trend of the changes of k_{nr} values.

where the values of ΔG_{CT}, $h\nu_i$, λ_o, and S are derived from the band-shape analysis of the CT fluorescence spectra (eqs 4 and 5) and those of the electronic coupling elements V_{AD} from the investigations of the radiative properties of the ^{1}CT states (eq 18). The discrepancies between the experimental rate constants k_{nr} and the values calculated from eq 21 for nicotinonitrile and dicyanobenzene derivatives are smaller than one order of magnitude (cf. Table 6) which may be regarded as satisfactory. For benzonitrile derivatives with relatively high energy of the CT state, however, most probably the ISC depopulation channel is dominant which results in much larger differences between the calculated and experimental k_{nr} values.

The obtained results illustrate that, similarly to electron transfer in contact radical ion pairs,[75] the Marcus theory can be used for at least a semiquantitative description of the electron transfer rate constants also in the intramolecular donor−acceptor systems when ISC processes can be neglected.

4. Concluding Remarks

Radiative and radiationless charge recombination processes exemplified respectively by the CT fluorescence and direct

radiationless charge recombination to the ground state have been studied in a series of N-bonded donor−acceptor derivatives of 3,6-di-*tert*-butylcarbazole containing benzonitrile, nicotinonitrile, or various dicyanobenzenes as an electron acceptor.

The results of the electrochemical measurements and the investigations of the solvent and temperature effects on the spectral position and band shape of the CT absorption and emission show a very good agreement (e.g., Figures 7, 12, and 13) between the two independent estimations of the energy levels of the ^{1}CT states based on the electrochemical E_{CT}(e) way and the photophysical E_{CT}(p) one[9,76]

$$E_{CT}(e) = E_{ox}(D) - E_{red}(A) + T\Delta S_o - \frac{e_o^2}{r_{AD}\,\epsilon} \qquad (22)$$

$$E_{CT}(p) = hc\tilde{\nu}_{flu} + \lambda_s + \lambda_i + \lambda_M \qquad (23)$$

where ΔS_o is a standard entropy change in the reaction (the values of $T\Delta S_o$ should be relatively small and can be neglected) and the last term in eq 22 corresponds to the coulombic stabilization energy (between the elementary charges e_o at the separation distance r_{AD}) in the radical ion pair (as forming an ICT state).

The analysis of the temperature dependence of the CT fluorescence profile and the bandwidth in a nonpolar environment suggests that the D−A carbazole derivatives, contrary to anthryl derivatives of aromatic amines,[28,29] do not undergo any significant low-frequency intramolecular nuclear motions (e.g., rotations) upon excitation. Thus, the twist angle between the donor and acceptor moieties in the emitting ^{1}CT state seems to be similar to that in the ground state. This hypothesis is strongly supported by the large values of the fluorescence rate constants (k_f) and the corresponding transition dipole moments (M). This finding clearly indicates a nonperpendicular conformation of the ^{1}CT state for all the D−A compounds studied (similarly to the aryl derivatives of aromatic amines[28] and various derivatives of biphenyl[12,30,31]).

The probabilities of the radiative electron transfer exemplified by the CT fluorescence can be correlated with the magnitude of the LCAO coefficient of the acceptor LUMO orbital at the position of the donor−acceptor bond (Figure 14 and Table 5). The large value (0.503) of the LCAO coefficient of the HOMO orbital at the carbazole nitrogen atom and the small one (0.153) of the corresponding coefficient of the LUMO orbital agree well with the dominant role of the electronic interactions between the emitting ^{1}CT state and the ground state.

The obtained results (Table 5 and Figure 15) illustrate that, similarly to electron transfer in contact radical ion pairs,[75] the Marcus theory can be used for the quantitative description of the radiationless electron transfer rate constants also in the intramolecular donor−acceptor systems when ISC processes can be neglected.

We hope that our comparative studies of the D−A compounds (the present paper and refs 27,28,73) will show a possibility to predict the photophysical behavior of the lowest excited intramolecular ^{1,3}CT states from the properties of the donor and acceptor subunits forming the D−A molecule.

Acknowledgment. This work was sponsored by Grant 3T09A12708 from the Committee of Scientific Research. Technical assistance from Mrs. A. Zielińska and Mrs. M. Gołębiewska is deeply appreciated.

Appendix

Blue Shift of the CT Absorption Bands. Description of the solvent effects on the absorption and fluorescence spectra is based on the Onsager concept[52] of the reaction field **R** created in the solution by a solute dipole moment $\vec{\mu}$ which is located at the center of the spherical cavity with the radius a_o

$$\mathbf{R} = \frac{2\vec{\mu}}{a_o^3}\,\frac{\epsilon - 1}{2\epsilon + 1} \qquad (A.1)$$

Onsager's theory provides a possibility to calculate the energy of equilibrium solvation of an ideal nonpolarizable dipole immersed in a dielectric continuum. Due to the nonequilibrium situation of the Franck−Condon states (as reached in the absorption or emission process), an approach to a solvatochromic data requires the function describing the solvation energy to be split into orientational (slow) and inductive (fast) components. Usually the Onsager reaction field is treated as the sum of two respective contributions $\mathbf{R}_{or}$ and $\mathbf{R}_{ind}$

$$\mathbf{R} = \mathbf{R}_{or} + \mathbf{R}_{ind} = \frac{2\vec{\mu}}{a_o^3}\left[\frac{\epsilon - 1}{2\epsilon + 1} - \frac{n^2 - 1}{2n^2 + 1}\right] + \frac{2\vec{\mu}}{a_o^3}\left[\frac{n^2 - 1}{2n^2 + 1}\right] \qquad (A.2)$$

This approach leads to the expressions for the reaction field in the Franck−Condon state reached either in the absorption or in the emission (cf. ref 48−53).

Taking also into account the energies required for the polarization of the solvent shell, the following expressions for the spectral shift of the absorption ($hc\Delta\tilde{\nu}_{abs}$) and fluorescence ($hc\Delta\tilde{\nu}_{flu}$) maxima can be obtained

$$hc\Delta\tilde{\nu}_{abs} = \frac{2\vec{\mu}_g(\vec{\mu}_e - \vec{\mu}_g)}{a_o^3}\left[\frac{\epsilon - 1}{2\epsilon + 1} - \frac{1}{2}\,\frac{n^2 - 1}{2n^2 + 1}\right] + \frac{\vec{\mu}_e(\vec{\mu}_e - \vec{\mu}_g)}{a_o^3}\left[\frac{n^2 - 1}{2n^2 + 1}\right] \qquad (A.3)$$

$$hc\Delta\tilde{\nu}_{flu} = \frac{2\vec{\mu}_e(\vec{\mu}_e - \vec{\mu}_g)}{a_o^3}\left[\frac{\epsilon - 1}{2\epsilon + 1} - \frac{1}{2}\,\frac{n^2 - 1}{2n^2 + 1}\right] + \frac{\vec{\mu}_g(\vec{\mu}_e - \vec{\mu}_g)}{a_o^3}\left[\frac{n^2 - 1}{2n^2 + 1}\right] \qquad (A.4)$$

which leads (with the assumption that the second terms in eqs A.3 and A.4 are nearly constant) to the familiar expressions (eqs 1 and 2) for the solvent induced shift of the absorption and fluorescence spectra. It should be noted that this formalism is principally applicable only for the spherical solutes with both $\vec{\mu}_g$ and $\vec{\mu}_e$ point dipole moments located in the center of the molecule.

If the dipole moment $\vec{\mu}$ is located eccentrically, the model should take into account the respective values of the reaction fields at the position of the dipole. A system for which such considerations can be performed without difficulty is an eccentric dipole in a spherical cavity, directed along the radius vector (with the distance r from the dipole to the cavity center). Such considerations have been first performed by Dekker[48] with the general conclusion that in the cavity center the value of the reaction field is independent of the dipole position. Contrary to that, at the position of the dipole, the reaction field **R** is enhanced by a factor ξ being a function of the solvent properties (ϵ or n^2) and the ratio r/a_o. The corresponding expression is

$$R = \frac{2\vec{\mu}}{a_o^3}\frac{z-1}{2z+1}\xi \quad \text{with}$$

$$\xi = \sum_{m=0}^{\infty} \frac{m^2(m+1)(2z+1)}{2(m+mz+z)}\left[\frac{r}{a_o}\right]^{(2m-2)} \quad \text{(A.5)}$$

where z is equal to ϵ or n^2 for $\mathbf{R}_{or}$ and $\mathbf{R}_{ind}$, respectively. The calculation of ξ performed for different values of z and r/a_o (cf. Figure 16) clearly establishes that the influence of z on the ξ is relatively small, but the effective value of $\mathbf{R}$ increases strongly with the eccentricity.

In our particular case the description of the reaction field of the bichromophoric molecule in the ground state is different than that in the excited state. The ground state dipole moment should be treated within the model including the corrections arising from its eccentric localisation. The excited state dipole moment, however, can be further considered in the classical Onsager model, due to the fact that if the dipole is localized in the center, the reaction field is uniform over the whole cavity. Following the mathematical procedures leading to eqs A.3 and A.4 one can obtain

$$hc\Delta\tilde{\nu}_{abs} = \frac{2\vec{\mu}_g(\vec{\mu}_e - \xi\vec{\mu}_g)}{a_o^3}\left[\frac{\epsilon-1}{2\epsilon+1} - \frac{1}{2}\frac{n^2-1}{2n^2+1}\right] + \frac{\vec{\mu}_e(\vec{\mu}_e - \vec{\mu}_g)}{a_o^3}\left[\frac{n^2-1}{2n^2+1}\right] \quad \text{(A.6)}$$

$$hc\Delta\tilde{\nu}_{flu} = \frac{2\vec{\mu}_e(\vec{\mu}_e - \vec{\mu}_g)}{a_o^3}\left[\frac{\epsilon-1}{2\epsilon+1} - \frac{1}{2}\frac{n^2-1}{2n^2+1}\right] + \frac{\vec{\mu}_g(\vec{\mu}_e - \xi\vec{\mu}_g)}{a_o^3}\left[\frac{n^2-1}{2n^2+1}\right] \quad \text{(A.7)}$$

From eq A.6 it becomes evident that the effects of the solvent polarity on the spectral position of the CT absorption depend on the relative values of the eccentric factor ξ and the ratio of the dipole moments $\vec{\mu}_e/\vec{\mu}_g$; the blue shift of the CT band is expected when $\xi > \vec{\mu}_e/\vec{\mu}_g$. On the contrary, the eccentricity effects which may influence the second term in eq A.7 should be negligible in the solvent dependence of fluorescence.

Similar considerations lead also to the description of the solvent-induced changes in the Stokes shift as well as in the energy gap ΔG_{CT} between the excited and the ground states. Changes in the Stokes shift correspond to the difference between $hc\Delta\tilde{\nu}_{abs}$ and $hc\Delta\tilde{\nu}_{flu}$

$$hc(\Delta\tilde{\nu}_{flu} - \Delta\tilde{\nu}_{abs}) = 2\frac{(\vec{\mu}_e - \vec{\mu}_g)^2}{a_o^3}\left[\frac{\epsilon-1}{2\epsilon+1} - \frac{n^2-1}{2n^2+1}\right] + (\xi-1)\frac{\vec{\mu}_g^2}{a_o^3}\left[\frac{\epsilon-1}{2\epsilon+1} - \frac{n^2-1}{2n^2+1}\right] \quad \text{(A.8)}$$

Similarly to fluorescence, the observed Stokes shift is mostly determined by the first term in the above equation which does not depend on the eccentricity; the slopes in the linearized plot of $hc(\Delta\tilde{\nu}_{flu} - \Delta\tilde{\nu}_{abs})$ vs solvent polarity function should be somewhat larger (ca. 10−20%) than those determined from the analysis of the CT fluorescence. It is observed indeed for the D−A compounds studied in this work.

The eccentricity effect is expected to be pronounced in the description of the changes of the energy gap between the excited state and the ground state. Such changes correspond to the differences in the equilibrated solvation energies of the dipoles

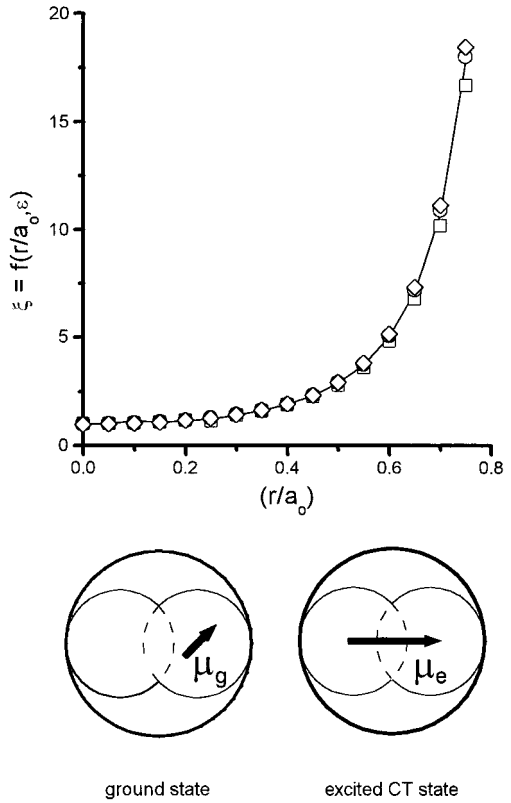

Figure 16. Illustration of the effects connected with a fact that the dipolar molecule cannot be approximated by the point dipole situated in the center of the cavity. The ground state dipole moment mostly determined by polar groups lying far from the center of the molecule leads to the increase of the effective Onsager reaction field[48] in the dipole position by a factor ξ and therefore induces the increase of the ground state solvation energies. In the CT excited state, however, in which the negative and positive ends of the electric dipole are localized nearly in the centers of the A and D subunits, respectively, the approximation of the spherical cavity with the dipole situated in its center seems to be better obeyed. The upper part shows the dependence (according to eq A.5) of ξ on the eccentricity of the dipole position (as related to the ratio of the distance r from the dipole to the cavity center and the Onsager's cavity radius a_o) and on the dielectric constants ϵ (squares, $\epsilon = 2$; circles, $\epsilon = 8$; and diamonds, $\epsilon = 32$).

$\vec{\mu}_e$ and $\vec{\mu}_g$

$$\Delta G_{CT} = \Delta G_{CT}^{vac} + \frac{\vec{\mu}_e^2}{a_o^3}\frac{\epsilon-1}{2\epsilon+1} - \xi\frac{\vec{\mu}_g^2}{a_o^3}\frac{\epsilon-1}{2\epsilon+1} \quad \text{(A.9)}$$

where ΔG_{CT}^{vac} is the energy of the CT state in the gas phase. The solvation energy of the ground state dipole moment is enlarged by a factor ξ; correspondingly the change of the ΔG_{CT} values with solvent polarity is smaller than that expected from the classical formulation

$$\Delta G_{CT} = \Delta G_{CT}^{vac} + \frac{\vec{\mu}_e^2}{a_o^3}\frac{\epsilon-1}{2\epsilon+1} - \frac{\vec{\mu}_g^2}{a_o^3}\frac{\epsilon-1}{2\epsilon+1} \quad \text{(A.10)}$$

According to eq A.10 the slopes of the linear relationship between the energy of the CT state and the solvent polarity function should be similar to terms $\vec{\mu}_e(\vec{\mu}_e - \vec{\mu}_g)/a_o^3$ obtained from the analysis of the solvent induced fluorescence shift. In fact, the experimental values of $(\vec{\mu}_e^2 - \vec{\mu}_g^2)/a_o^3$ for the studied D−A compounds are smaller somewhat than the $\vec{\mu}_e(\vec{\mu}_e - \vec{\mu}_g)/a_o^3$, suggesting that eq A.9 is more accurate for the quantitative description.

In summary, the description of the solvent polarity effects on the charge transfer processes may be improved by taking into considerations the eccentricity effect. In our case this effect can be simply applied for the D−A systems with cyano group(s) in the meta or para position with respect to the donor−acceptor bond (e.g. CNP, CBM, CBP, CIM, or CPM). More complicated is the situation for the compounds with two cyano groups, one of them being in the ortho position with respect to the donor−acceptor bond (e.g., CIP, CPO, or CTO). In such cases, one of the group is far from the cavity center and should be treated as described above. The second one (in the ortho position, i.e., located nearer to the cavity center) should be treated "classically" or with the smaller value of ξ. Moreover, the direction of the dipole moment of this particular group with regard to the excited state dipole moment induces already (according to eq A.3) a small blue shift in the absorption spectra (in the same way as for CBO or CNO). Thus, both cyano groups in CPO, CTO, and CIP are expected to cause the changes in the same direction, but the quantitative estimation of both contributions seems to be rather difficult. Moreover, for these derivatives the blue shift in the absorption spectra should be more pronounced as compared for example with CNP or CPM, which is observed indeed.

References and Notes

(1) Lippert, E.; Lüder, W.; Boss, H. In *Advances in Molecular Spectroscopy*; Mangini, A., Ed.; Pergamon Press: Oxford, 1962; p 443.

(2) Rotkiewicz, K.; Grellmann, K. H.; Grabowski, Z. R. *Chem. Phys. Lett.* **1973**, *19*, 315.

(3) Chandross, E. A. In *The Exciplex*; Gordon, M., Ware, W. R., Eds.; Academic Press: New York, 1975; p 187.

(4) Grabowski, Z. R.; Rotkiewicz, K.; Siemiarczuk, A.; Cowley, D. J.; Baumann, W. *Nouv. J. Chim.* **1979**, *3*, 443.

(5) Visser, R. J.; Varma, C. A. G. O.; Konijnenberg, J.; Bergwerf, P. *J. Chem. Soc., Faraday Trans. 2* **1983**, *79*, 347.

(6) Cazeau-Dubroca, C.; Ait-Lyazidi, S.; Cambou, P.; Peirigua, A.; Cazeau, Ph.; Pesquer, M. *J. Phys. Chem.* **1989**, *93*, 2347.

(7) Zachariasse, K. A.; von der Haar, T.; Hebecker, A.; Leihos, U.; Kühnle W. *Pure Appl. Chem.* **1993**, *65*, 1745.

(8) Sobolewski, A. L.; Domcke, W. *Chem. Phys. Lett.* **1996**, *250*, 428.

(9) Grabowski, Z. R.; Dobkowski, J. *Pure Appl. Chem.* **1983**, *55*, 245.

(10) Rullière, C.; Grabowski, Z. R.; Dobkowski, J. *Chem. Phys. Lett.* **1987**, *137*, 408.

(11) Herbich, J.; Grabowski, Z. R.; Wójtowicz, H.; Golankiewicz, K. *J. Phys. Chem.* **1989**, *93*, 3439.

(12) Herbich, J.; Waluk, J. *Chem. Phys.* **1994**, *188*, 247, and references cited therein.

(13) Rettig, W. *Angew. Chem., Int. Ed. Engl.* **1986**, *25*, 971.

(14) Lippert, E.; Rettig, W.; Bonačić-Koutecký, V.; Heisel, F.; Miehé, J. A. In *Advances in Chemical Physics*; Prigogine, I., Rice, S. A., Eds.; Wiley: New York, 1987, p 1.

(15) Rettig, W. In Topics in Current Chemistry; Mattay, J., Ed.; Springer: Berlin, 1994, p 253.

(16) De Lange, M. C. C.; Thorn Leeson, D.; van Kuijk, K. A. B.; Huizer, A. H.; Varma, C. A. G. O. *Chem. Phys.* **1993**, *188*, 247.

(17) Von der Haar, Th.; Hebecker, A.; Il'ichev, Y.; Jiang, Y.-B.; Kühnle, W.; Zachariasse, K. A. *Recl. Trav. Chim. Pays-Bas* **1995**, *114*, 430.

(18) Rettig, W.; Zander, M. *Ber. Bunsen-Ges. Phys. Chem.* **1983**, *87*, 143.

(19) Dobkowski, J.; Grabowski, Z. R.; Paeplow, B.; Rettig, W.; Koch, K. H.; Müllen, K.; Lapouyade, R. *New J. Chem.* **1994**, *18*, 525 and references cited therein.

(20) Okada, T.; Fujita, T.; Kubota, M.; Masaki, S.; Mataga, N.; Ide, R.; Sakata, Y.; Misumi, S. *Chem. Phys. Lett.* **1972**, *14*, 563.

(21) Siemiarczuk, A.; Grabowski, Z. R., Krówczyński, A.; Asher, M.; Ottolenghi, M. *Chem. Phys. Lett.* **1977**, *51*, 315.

(22) Siemiarczuk, A.; Ware, W. R. *J. Phys. Chem.* **1987**, *91*, 3677.

(23) Okada, T.; Mataga, N.; Baumann, W.; Siemiarczuk A. *J. Phys. Chem.* **1987**, *91*, 4490.

(24) Mataga, N.; Nishikawa, S.; Asahi, T.; Okada, T. *J. Phys. Chem.* **1990**, *94*, 1443 and references cited therein.

(25) Tominaga, K.; Walker, G. C.; Jarzęba, W.; Barbara, P. F. *J. Phys. Chem.* **1991**, *95*, 10475.

(26) Tominaga, K.; Walker, G. C.; Kang, T. J.; Barbara, P. F.; Fonseca, T. *J. Phys. Chem.* **1991**, *95*, 10485.

(27) Herbich, J.; Kapturkiewicz, A. *Chem. Phys.* **1991**, *158*, 143.

(28) Herbich, J.; Kapturkiewicz, A. *Chem. Phys.* **1993**, *170*, 221 and references cited therein.

(29) Onkelinx, A.; De Schryver, F. C.; Viaene, L.; Van der Auweraer, M.; Iwai, K.; Yamamoto, M.; Ichikawa, M.; Masuhara, H.; Maus, M.; Rettig, W. *J. Am. Chem. Soc.* **1996**, *118*, 2892 and references cited therein.

(30) Tamai, N.; Yamazaki, Y.; Masuhara, H.; Mataga, N. *Chem. Phys. Lett.* **1984**, *104*, 485.

(31) Van Damme, W.; Hofkens, J.; De Schryver, F. C.; Ryan, T. G.; Rettig, W.; Klock, A. *Tetrahedron* **1989**, *45*, 4693.

(32) Rettig, W.; Zander, M. *Chem. Phys. Lett.* **1982**, *87*, 229.

(33) Mulliken, R. S.; Person, W. B. *Molecular Complexes. A Lecture and Reprint Volume*; Wiley: New York, 1969.

(34) Beens, H.; Weller, A. In *Organic Molecular Photophysics*; Birks, B. J., Ed.; Wiley: New York, 1975; Vol. 2, p 159.

(35) Nowacki, J., in preparation.

(36) Jasny, J. *J. Lumin.* **1978**, *17*, 143.

(37) Velapoldi, R. A. Natl. But. Std. 378, Proc. Conf. NBS, Gaithersburg **1972**, p231.

(38) Karpiuk, J.; Grabowski, Z. R. *Chem. Phys. Lett.* **1989**, *160*, 451.

(39) Marquardt, D. W. *J. Soc. Ind. Appl. Math.* **1963**, *11*, 431.

(40) Kapturkiewicz, A.; Grabowski, Z. R.; Jasny, J. *J. Electroanal. Chem.* **1990**, *279*, 55.

(41) Kapturkiewicz, A. *J. Electroanal. Chem.* **1993**, 348, 283.

(42) Bigelow, R. W.; Johnson, G. E. *J. Phys. Chem.* **1977**, 66, 4861.

(43) Gudipati, M. S.; Daverkausen, J.; Maus, M.; Hohlneicher, G. *Chem. Phys.* **1994**, *186*, 289 and references cited therein.

(44) Thulstrup, E. W.; Brodersen, A.; Rasmussen, S. K. *Polycyclic Aromatic Hydrocarbons*, in press.

(45) *DMS UV Atlas of Organic Compounds*; Verlag Chemie: Weinheim; Butterworths: London, 1966.

(46) *The Sadtler Handbook of Ultraviolet Spectra*; Sadtler Research Laboratory: Philadelphia, 1979.

(47) Chiba, K.; Aihara, J.-I.; Araya, K.; Matsunaga, Y. *Bull. Chem. Soc. Jpn.* **1980**, *53*, 1703.

(48) Böttcher, C. J. F. In Theory of Electric Polarization, Van Belle, O. C., Bordewijk, P., Rip, A., Eds.; Elsevier: Amsterdam, 1973; Vol. I.

(49) Lippert, E. Z. *Naturforsch.* **1955**, *A10*, 541.

(50) Mataga, N.; Kaifu, Y.; Koizumi, M. *Bull. Chem. Soc. Jpn.* **1955**, *28*, 690.

(51) Liptay, W. In *Excited States*; Lim, E. C., Ed.; Academic Press: New York, 1974; p 129.

(52) Onsager, L. *J. Am. Chem. Soc.* **1936**, *58*, 1486.

(53) McRae, E. G. *J. Phys. Chem.* **1957**, *61*, 562.

(54) Kapturkiewicz, A. *Chem. Phys.* **1992**, *166*, 259.

(55) Ambroese, J. F.; Carpentier, L. L; Nelson, R. F. *J. Electrochem. Soc.* **1975**, *122*, 876.

(56) Bloor, J. E.; Gilson, B. R.; Shillady, D. D. *J. Phys. Chem.* **1967**, *71*, 1238.

(57) Marcus, R. A. *J. Phys. Chem.* **1989**, *93*, 3078 and references cited therein.

(58) Gould, I. R.; Young, R. H.; Miller, L. J.; Albrecht, A. C.; Farid, S. *J. Am. Chem. Soc.* **1994**, *116*, 8188.

(59) Cortes, J.; Heitele, H.; Jortner, J. *J. Phys. Chem.* **1994**, 98, 2527 and references cited therein.

(60) Auty, A. R.; Jones, A. C., Phillips, D. *Chem. Phys.* **1986**, 103, 163.

(61) Bader, J. S.; Berne, B. J. *J. Chem. Phys.* **1996**, *104*, 1293.

(62) Marcus, R. A. *J. Chem. Phys.* **1965**, *43*, 679.

(63) Birks, J. B. In *Photophysics of Aromatic Molecules*; Wiley: New York, 1978; p 48.

(64) Bixon, M.; Jortner, J.; Verhoeven, J. W. *J. Am. Chem. Soc.* **1994**, *116*, 7349 and references cited therein.

(65) Dogonadze, R. R.; Kuznetsov, A. M.; Marsagishvili, T. A. *Electrochim. Acta* **1980**, *25*, 1.

(66) McConnell, H. M. *J. Chem. Phys.* **1956**, *24*, 632, 764.

(67) Bloor, J. E.; Gilson, B. R.; Shillady, D. D. *J. Phys. Chem.* **1967**, *71*, 1238.

(68) Klöpffer, W.; Kaufmann, G.; Naudorf, G. *Z. Naturforsch.* **1971**, *A26*, 897.

(69) Barański, A.; Fawcett, W. R. *J. Electroanal. Chem.* **1979**, *100*, 185.

(70) Barassin, J.; Lumbrosso, H. *Bull. Soc. Chim. France* **1961**, 492.

(71) Liptay, W.; Eberlain, W.; Weindenberg, H.; Elflein, O. *Ber. Bunsen-Ges. Phys. Chem.* **1967**, *71*, 548.

(72) Avendaño, C.; Espada, M.; Ocaña, B.; Garcia-Granda, S.; del Rosario Diaz, M.; Tejerina, B.; Gómez-Beltrán, F.; Martinez, A.; Elguero. J. *J. Chem. Soc., Perkin Trans. 2*, **1993**, 1547.

(73) Herbich, J.; Kapturkiewicz, A.; Nowacki, J. *Chem. Phys. Lett.* **1996**, *262*, 633.

(74) Efrima, S.; Bixon, M. *Chem. Phys. Lett.* **1974**, *25*, 341.

(75) Gould, I. R.; Noukakis, D.; Gomez-Jahn, L.; Young, R. H.; Goodmann, J. L.; Farid, S. *Chem. Phys.* **1993**, *176*, 439.

(76) Weller, A. *Z. Phys. Chem. (Münich)* **1982**, *133*, 93.